Atomic Force Microscope Measurements of Long-Range Forces Near Lipid-Coated Surfaces in Electrolytes

W. Xu,* B. L. Blackford,* J. G. Cordes,* M. H. Jericho,* D. A. Pink,# V. G. Levadny,§ and T. Beveridge¶
*Department of Physics, Dalhousie University, Halifax, Nova Scotia B3H 3J5, Canada; #Department of Physics, St. Francis Xavier University, Antigonish, Nova Scotia B2G 2W5, Canada; §Departamento de Ciencies Experimentals, Universidad Jaume 1, 12080 Castellon, Spain; and ¶Department of Microbiology, University of Guelph, Guelph, Ontario N1G 2W1, Canada

ABSTRACT The interaction of DMPC (L-α-dimyristoyl-1,2-diterradecanoyl-sn-glycero-3-phosphocholine, $C_{36}H_{72}NO_8P$) lipid-coated Si_3N_4 surfaces immersed in an electrolyte was investigated with an atomic force microscope. A long-range interaction was observed, even when the Si_3N_4 surfaces were covered with nominally neutral lipid layers. The interaction was attributed to Coulomb interactions of charges located at the lipid surface. The experimental force curves were compared with solutions for the linearized as well as with exact solutions of the Poisson-Boltzmann equation. The comparison suggested that in 0.5 mM KCl electrolyte the DMPC lipids carried about one unit of charge per 100 lipid molecules. The presence of this surface charge made it impossible to observe an effective charge density recently predicted for dipole layers near a dielectric when immersed in an electrolyte. A discrepancy between the theoretical results and the data at short separations was interpreted in terms of a decrease in the surface charge with separation distance.

INTRODUCTION

Atomic force microscopy (AFM) has opened the way for the measurement of interaction forces between biological components such as proteins and lipids on a local scale, and the distance dependence of this interaction can now be determined with considerable sensitivity. In an electrolyte the long-range interaction at distances greater than 5 nm is generally dominated by electrostatic forces, whereas a variety of interactions such as van der Waals, solvation, and hydration forces also determine the interaction at short range. The electrostatic interaction has its origin in charges that tend to be present on surfaces immersed in an electrolyte. The screening of these charges by the electrolyte ions then leads to an osmotic pressure contribution to the interaction. Considerable theoretical work on this type of interaction was published in the past (Verwey and Overbeek, 1948; Parsegian and Gingell, 1972; Honig and Mul, 1971), and an excellent review of the theory and experiments on the interaction between charged surfaces across an electrolyte is given by Israelachvili (1985). The first AFM measurements of this long-range electrostatic force were reported by Weisenhorn et al. (1992). Detailed measurements of the force as a function of aqueous electrolyte concentration were reported by Butt (1991a), who also made a theoretical study of the interaction (1991b). A very thorough AFM study of the force between a silicon nitride tip and a silicon nitride surface as a function of salt concentration and as a function of electrolyte pH was made by Drummond and Senden (1994) and by Senden and Drummond (1995). These studies showed that the AFM has sufficient sensitivity to give detailed information about the interaction forces between surfaces in an electrolyte. This subject was recently reviewed by Butt (1995). Comparison of the measured forces with theoretical models have generally followed simple Derjaguin-Landau-Verwey-Overbeek (DLVO) theory.

Interfaces between a dielectric, such as the hydrophobic interior of a membrane, and an electrolyte are of special interest in biology. In the case of a lipid, the interface can have a complex structure and the hydrophilic headgroups may carry a charge or a dipole moment. The headgroups form an interfacial zone that is defined by the hydrophobic fatty acid tails on the one hand and by the beginning of the bulk electrolyte region on the other. In many systems the electrolyte may move freely through this interface zone; the interface is known as a soft interface. Belaya et al. (1994a) recently showed that for soft interfaces of this type, the electric potential in the solution is determined by both surface charges and surface dipoles. Thus a surface with zero net charge but nonzero dipole moment perpendicular to the surface will appear to have an effective charge that depends on the dipole density, the Debye screening length, and the width of the interface region. These effective charges should thus make a contribution to the force between an AFM tip and a lipid-coated substrate if both are immersed in an electrolyte. In addition to this effective charge interaction, Belaya et al. (1987), using a model that represented the dynamically hydrogen-bonded clusters in an aqueous medium by a nonlocal permittivity, showed that it would change the charge interaction over a characteristic distance. These nonlocal effects can be expected to contribute significantly to the interaction between surfaces for distances below ~2 nm. Below a separation of ~2 nm the total interaction between surfaces can thus include the familiar hydration, solvation, and van der Waals forces, as

Received for publication 15 August 1996 and in final form 12 December 1996.

Address reprint requests to Dr. M. H. Jericho, Department of Physics, Dalhousie University, Halifax, Nova Scotia B3H 3J5 Canada. Tel.: 902-494-2337; Fax: 902-494-5191; E-mail: manfred.jericho@dal.ca.

0006-3495/97/03/1404/10 $2.00

well as local and nonlocal contributions from surface charges and surface dipoles.

This paper describes measurements of the force between silicon nitride tips and lipid-coated surfaces in the presence of aqueous electrolytes. Our objective was to measure the long- and short-range interaction and examine the extent to which information about surface charges (real or effective) can be obtained from a comparison of the data with theoretical models.

MATERIALS AND METHODS

DMPC (L-α-dimyristoyl-1,2-diterradecanoyl-sn-glycero-3-phosphocholine, $C_{36}H_{72}NO_8P$) was purchased from Sigma Chemical Company (St. Louis, MO). To spread lipid molecules onto substrates forming single or multiple bilayers, we first made giant vesicles of DMPC with a procedure similar to that described by Rädler et al. (1994). Lipid was dissolved in 10 mg/ml chloroform/methanol (2:1). The lipid solution was dried on a Teflon disk and desiccated under vacuum for 2 h. The disk was then soaked in pure water for 24 h, and vesicles were detached from the Teflon surface. A drop of this vesicle suspension (~0.5 mg/ml) was spread onto the Si_3N_4 substrate and left to stay for a few minutes. The sample was then dried in air and mounted on the sample stage of the atomic force microscope. The tip was coated with lipid in a similar way. The presence of lipid on the tip was indicated by the absence of the jump to contact behavior when a Si_3N_4 sample was brought close to the coated tip. The procedure for coating the tip was repeated until the coating criteria discussed above were met.

Theoretical models for the interaction of charged surfaces in an electrolyte have generally been solved only for symmetrical surfaces, i.e., surfaces of the same material and therefore likely to carry the same charge. As substrates for the force measurements we therefore used the Si_3N_4-coated glass support plates for the Si_3N_4 cantilevers. Before each use the surface was treated with 20% analytical grade HCl, followed by rinsing in distilled water. Topographic scans of these surfaces with sharp tips suggested a surface roughness of less than 10-nm amplitude.

Force measurements were performed with an optic fiber interferometer-type microscope. V-shaped microfabricated Si_3N_4 cantilevers with pyramidal tips were employed for the measurements. Reliable force measurement at large separation distances are only possible if stray reflections of the laser light from the substrate surface can be eliminated. To achieve this we glued a small piece (~70 μm^2 in area) of metal foil to the end of the cantilevers and completely eliminated these spurious background signals. An important parameter in any AFM force measurement is the cantilever force constant. It was shown by Cleveland et al. (1993) that for cantilevers with uniform shape, reliable calibration can be obtained through a measurement of the cantilever resonance frequency. Cantilevers with foils epoxied to their ends are more compex elastic systems, and force constant determination from resonance frequencies becomes very unreliable. We therefore calibrated our cantilevers by observing the cantilever deflections when a known force was applied to the tip region of the cantilevers. The force constants of the 200-μm-long cantilevers were determined with this method to be 0.14 ± 10% N/m.

For a force measurement the substrate is mounted on a piezoelectric stage that moves the sample toward or away from the tip. Typical speeds used were 200 nm/s, although we always varied the speed over a large range to ensure that the results were not speed dependent. The force determined by multiplying the cantilever deflection with the spring constant of the cantilever was plotted as a function of the position of the piezoelectric stage. The force curves were first recorded on a digital oscilloscope (LeCroy9420), and the data were then transferred to a computer. A thousand points were transferred within each cycle, so that an approach curve contained 500 points. With single-trace data collection, the resolution in force was on the order of 0.04 nN, which corresponded to a deflection of ~3 Å. With averaging over multiple curves, this resolution could be improved to less than 0.02 nN. The tip-sample distance was extracted from the raw data by allowing for the deflection of the cantilevers as described by Ducker et al. (1991). Force measurements were performed at 27°C and therefore above the gel-fluid transition temperature of the DMPC. Measurements were made in both pure water and various concentrations of KCl solutions. The pH values of these solutions were ~5.7. The water for the electrolyte was of nano-pure grade, and analytical grade KCl was used.

RESULTS

Fig. 1 shows force curves for approach and retraction for a Si_3N_4 tip over a Si_3N_4 surface. Fig. 1 *a* shows the force cycle for pure water, and Fig. 1 *b* represents the force variation for 0.5 mM KCl electrolyte. All force curves presented are single traces unless indicated otherwise. With pure water the interaction forces on the tip during approach either cancel or are below the 0.04-nN noise level, and the approach curves were flat down to about 7 nm from the surface. At closer approach the cantilever becomes unstable and the tip jumps into contact with the Si_3N_4 substrate. As the sample is raised further after tip contact, the deflections of the cantilever and sample surface are essentially equal and the force curves are straight. The withdraw trace again starts out as a straight line but is slightly displaced from the approach curve because of piezo hysteresis (<1 nm). As the surface is withdrawn further, the force on the tip becomes negative because of strong adhesion effects, and the tip is not released from the surface until the surface has been withdrawn by a substantial distance. When the pure water is replaced by 0.5 mM KCl electrolyte solution at a pH of about 5.7, a long-range repulsive force is measured as shown in Fig. 1 *b*. At about 5 nm from the surface the tip again becomes unstable and jumps into contact with the surface. On retraction, adhesion forces, weaker than for the

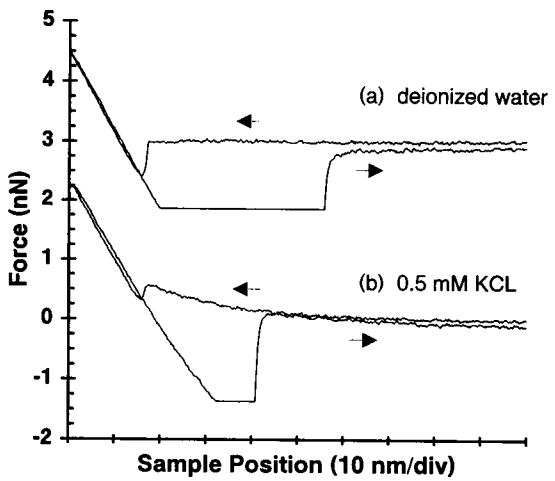

FIGURE 1 Force as a function of sample position between a silicon nitride tip and a silicon nitride sample in pure water (*a*) and in 0.5 mM KCl (*b*). Curves (*a*) are shifted up by 3 nN for clarity. Both approach of the sample to the tip and retraction are shown. The small shift in the contact lines of the curve was due to the piezo scanner's hysteresis and is present on every curves. The large hysteresis during retraction, on the other hand, shows that a strong adhesion is acting between the tip and the substrate.

pure water case, are again observed. These results are very similar to those reported by Butt (1991b) and by Senden and Drummond (1995).

To measure the interaction of the Si_3N_4 tip with lipid films, we deposited the lipid as described above. Fig. 2 is an AFM image of DMPC lipid bilayers collapsed from DMPC vesicles and spread over a silicon nitride substrate. There are one, two, and three bilayer doublets present on this image, and each double layer (four DMPC molecules thick) is about 9.1 nm high. The image was recorded under water with a force of less than 6 nN. Scan speeds from 700 to 7000 nm/s were used, and for that range images were reproducible and image contrast did not depend on scan speed.

Two basic approaches were used to measure the interaction between lipid and Si_3N_4. In one method lipid was deposited on a Si_3N_4 substrate as described above. After a topographic scan the Si_3N_4 tip was placed over a suitable lipid double layer and force curves were obtained. Fig. 3 *a* is an example of a single force cycle over lipid in 2 mM KCl electrolyte. The main feature is the presence of a repulsive force and the absence of a tip instability signature. Furthermore, no significant adhesion effects were observed on withdrawal. The maximum force of 2.9 nN that the tip applied to the lipid surface was apparently not enough to produce tip adhesion. Fig. 3 *b* shows an average of five such force cycles and gives an indication of the noise level that can be achieved and the general good reproducibility of the data on successive tip excursions. When experiments were repeated with new surfaces and electrolyte, the same general features were observed but the magnitudes of the repulsive force varied on occasion by as much as 50%. We attribute this to a variation of the surface charge that is responsible for the repulsive forces, and in the comparison with theoretical models discussed below we treated the surface charge as an adjustable parameter. As for the Si_3N_4–Si_3N_4 case, the higher force regions of the force curves in Fig. 3 are again straight and thus suggest that the tip is contacting a rigid surface.

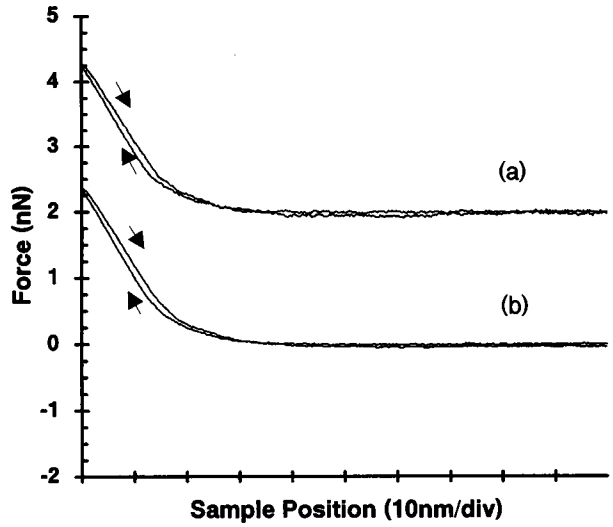

FIGURE 3 Force as a function of sample displacement between a silicon nitride tip and a lipid bilayers adsorbed on a silicon nitride substrate, in 2 mM KCl. (*a*) Single approach and retraction curves; (*b*) average of five individual approach and retraction curves. Curves show a repulsive force, no tip instability, and a linear hard-surface contact behavior.

A particularly significant observation was that the magnitude and range of the repulsive component did not depend on whether the tip was placed over a single bilayer doublet or over as many as four bilayer doublets. This observation strongly suggests that the charges responsible for the repulsive interaction with lipid-coated surfaces reside at the lipid-electrolyte interface and not just on the Si_3N_4 substrate.

In the second method lipid was deposited on the tip in the manner described above, and the interaction of the lipid-coated tip with a clean Si_3N_4 substrate was determined. In this case it is difficult to ascertain how many lipid layers are covering the tip. A series of experiments were performed in which a deliberate excess of lipid was deposited. In approach curves to a Si_3N_4 surface such tips produced no

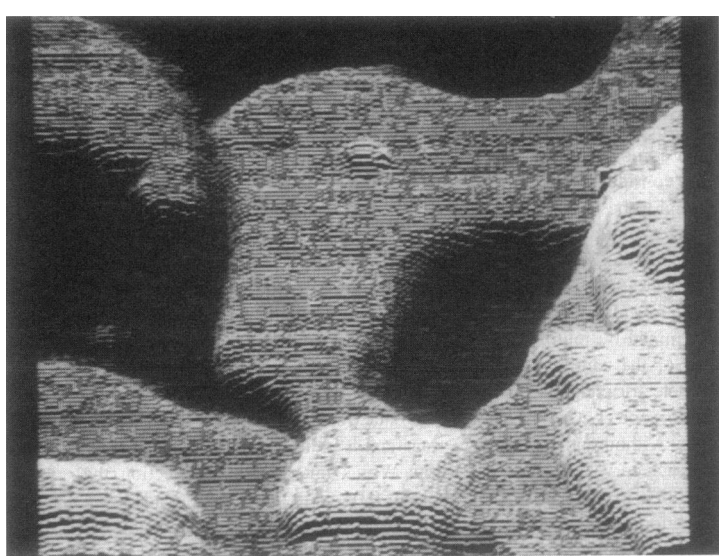

FIGURE 2 AFM image of DMPC lipid bilayers from DMPC vesicles and spread over silicon nitride substrate. The image is height shaded, and height steps correspond to one, two, and three lipid double bilayers (~4.5 nm for one bilayer). Imaging was conducted in pure water with a force of ~4 nN. Image size is 1400 nm × 1700 nm.

cantilever instability. An example of such an approach curve is shown in Fig. 4. In pure water no long-range interaction is observed, and at the sample position indicated by the vertical arrow, the coated tip appears to make contact with the Si_3N_4 substrate. At shorter distances the force curve lies considerably below the line that is expected for contact between hard surfaces (the *dotted line* in Fig. 4), and the curve is characteristic for the behavior of an elastically soft medium. In addition, as shown in Fig. 4, these curves showed considerable adhesion effects on retraction. Force curves for tips that were deliberately coated with excess lipid often became irregular during a measurement cycle. Subsequent imaging of the area under the tip then generally revealed a deposit that was most likely lipid material that was removed from the tip during the approach and retraction measurements. Observation of such deposits thus showed that multilayers of lipid on the tip did not have good mechanical stability. For the interaction measurement of a lipid-coated tip with a Si_3N_4 substrate we considered only those cases in which the contact line was close to that expected for hard surfaces (as was observed for clean tips against single or multiple bilayers in the first method) and in which no cantilever instability was observed for pure water or electrolyte. Fig. 5 is an example of such a set of force curves. Fig. 5 *a* is for pure water, and Fig. 5 *b* is for the 0.5 mM KCl electrolyte. The curve for pure water is essentially flat, except for a 1- to 2-nm-wide region near contact. The slight rounding of the force curve before the hard-surface slope is reached may suggest a small compression of the lipid coating on the tip. No cantilever instability and essentially no tip adhesion and hence excellent force reversibility are observed. For the interaction in the presence of the electrolyte, Fig. 5 *b* shows a long-range repulsion, good reversibility, and no cantilever instability.

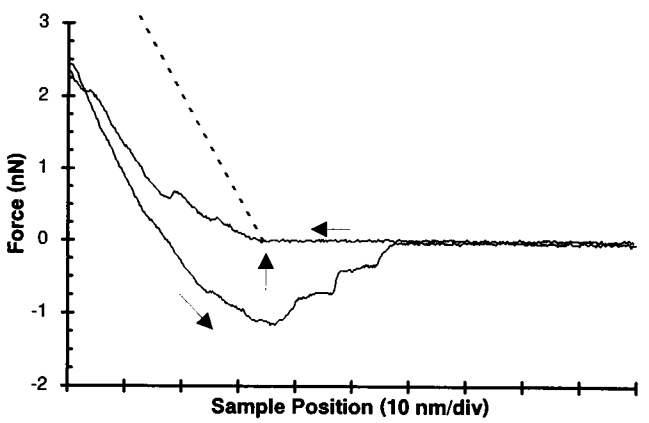

FIGURE 4 Interaction force as a function of sample position for a Si_3N_4 surface facing a Si_3N_4 tip coated with many DMPC lipid layers in pure water. After the Si_3N_4 surface has made contact with the lipid (*vertical arrow*), the repulsive force on the tip increases as the sample is moved further in the tip direction, but the force increase is considerably smaller than that expected (*dotted line*) from contact between hard surfaces. The slow increase in the repulsive force is evidence that the lipid layers on the tip are being deformed as the force increases. On retraction the force curve shows large adhesion effects.

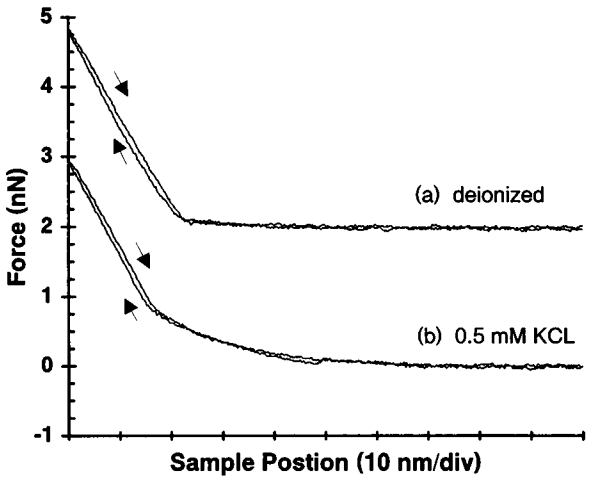

FIGURE 5 Force as function of sample position for a lipid-coated tip and a Si_3N_4 surface (*a*) in pure water and (*b*) in 0.5 mM KCl electrolyte. The curves are characterized by an absence of a tip instability, a long-range repulsive force when electrolyte is present, and an absence of significant adhesion, so that good reversibility between approach and retraction is obtained.

Measurements of the interaction between two lipid-coated surfaces proved much more difficult. Although the tip can be coated with lipid as described above, confirmation of a coating at the apex of a tip when lipid is facing lipid is more difficult to obtain. The only method at our disposal was the adhesion test, which is suggested by the above two results. After depositing lipid on the tip by the methods described above, an approach under pure water was made over a clean Si_3N_4 surface. If no adhesion was observed, then it was assumed that the tip was coated with lipid, although the number of lipid layers was not known. A lipid-coated Si_3N_4 surface was then imaged with this tip under minimum force conditions and the interaction over lipid islands was determined. Although care was taken to always image under minimum force conditions, we cannot be sure that the clean Si_3N_4 surfaces (such as the tip in the Si_3N_4-lipid experiment or the bare substrate region in the lipid-lipid experiment) were free from individual lipid molecule contamination, because isolated molecules cannot be imaged with the AFM. The significance of such potential contamination for the force curves is also unknown. An example of the interaction between lipid-coated surfaces according to the criteria outlined above is shown in Fig. 6. Under pure water as shown in Fig. 6 *a*, the force curves are again essentially independent of separation distance. The force curves in Fig. 6 *b* for the 0.5 mM KCl electrolyte show a clear repulsive force component, although it is somewhat smaller than for the asymmetrical experiment.

For each of the above tip and sample arrangements, we performed a sequence of measurements at salt concentrations from 0.1 to 50 mM. We observed that they all had the general characteristics of curves measured in 0.5 mM. An increase in electrolyte concentration caused a reduction in the Debye length and therefore a reduction in the range of

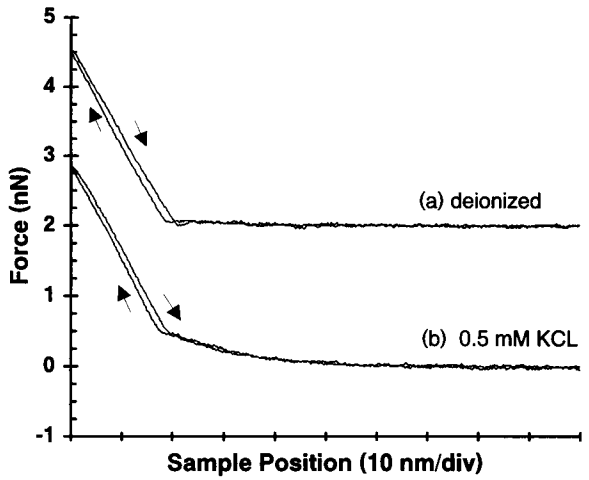

FIGURE 6 Force between a lipid-covered silicon nitride tip and a lipid bilayer adsorbed on a silicon nitride substrate (*a*) in pure water and (*b*) in 0.5 mM KCl. Adhesion between lipids is nearly absent on retraction.

the repulsive force. Fig. 7 shows an example of approach curve results for the three combinations of surfaces at a salt concentration of 50 mM KCl.

DISCUSSION

All three combinations of surfaces described above show a long-range repulsive force when measurements are made while surfaces are immersed in electrolyte. This long-range repulsion is generally attributed to charges that reside on the surfaces. The origin of these charges can be either the dissociation of surface molecular groups or the adsorption of ions to the surfaces. Chemical reactions that can produce charged Si_3N_4 surfaces have been discussed by Senden and Drummond (1995), who suggested that the main contribution to the charge on Si_3N_4 in an aqueous medium comes from silanol and silylamine surface groups. Their force measurements on Si_3N_4 surfaces showed that in the absence of a background electrolyte, the Si_3N_4 surface is close to being electrically neutral for pH values ranging from 6 to 8.5, so that the silanol and silylamine surface groups are present in approximately equal density. As will be shown below, in an electrolyte counter-ion binding can produce a net surface charge on nominally neutral surfaces. These surface charges will be screened, and the electrostatic potential away from a surface can be obtained by solving the Poisson-Boltzmann equation.

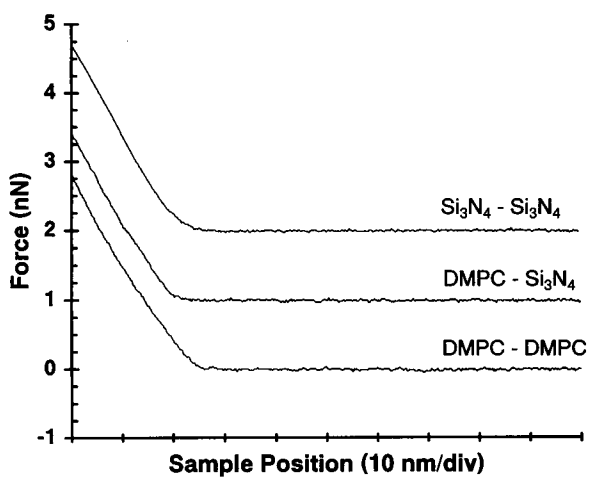

FIGURE 7 Force as function of sample position for the three combinations of surfaces studied in 50 mM KCl electrolyte. The repulsive force is very short-range for all three surface combinations and is on the order of the Debye length of 1.4 nm.

If the interaction energy per unit area between flat plates a distance D apart is $w(D)$ then in the Derjaguin approximation the force between two bodies with closest distance of separation, H, is given by (White, 1983)

$$F(H) = \frac{2\pi}{(\lambda_1\lambda_2)^{1/2}}\, w(H). \tag{1}$$

In Eq. 1 λ_1 and λ_2 involve the radii of curvature of the interacting surfaces. For a sphere of radius R and the closest distance H away from a flat plate, the force is given by

$$F(H) = 2\pi R w(H). \tag{2}$$

The interaction energy, $w(H)$, can be calculated by a numerical solution of the nonlinear Poisson-Boltzmann equation or by the closed-form calculation of Honig and Mul (1971). A more physically transparent form for the dependence of the interaction force on quantities like the Debye length and surface charges, particularly for asymmetrically charged surfaces, can be obtained if the linearized form of the equation is considered. In that case the solutions are valid if $e\psi/k_bT \ll 1$, where ψ is the surface potential.

For the situation where conventional electrostatics applies, the interaction force is given by (Levatny et al., 1996)

$$F_l(H) = \frac{2\pi R}{\epsilon_0\epsilon_S}\left\{\frac{1}{k}\frac{1}{sh(kH)}\left[(\sigma^2_{1k} + \sigma^2_{2k})e^{-kH} + 2\sigma_{1k}\sigma_{2k}\right]\right\}. \tag{3}$$

In Eq. 3 σ_{ik} are effective charges on the substrate and tip, ϵ_s is the permittivity of the electrolyte, ϵ_o is the permittivity of free space, and k is the inverse Debye length.

For a lipid layer such as DMPC, surface dipoles with a dipole density, ν, and possibly a surface charge with a density σ, exist at the electrolyte interface. If the electrolyte can penetrate the region between the hydrocarbon tails and the lipid surface, then the electrostatic potential in the electrolyte can be written in a Gouy-Chapman form if an effective charge σ_k is defined where (Belaya et al., 1994a):

$$\sigma_k = [\sigma\, ch(kl) + \nu\, ksh(kl)]e^{-kl}. \tag{4}$$

In Eq. 4 point charges and point dipoles are assumed to exist a distance l from the dielectric boundary.

If the electrolyte is described by a nonlocal permittivity function, then an additional force arises that is given by

(Levatny et al., 1996)

$$F(H) = \frac{2\pi R}{\varepsilon_0 \varepsilon_S}\left\{\frac{C_1}{n}\frac{1}{N(nH)} \cdot \left[(\sigma^2_{1n} + \sigma^2_{2n})\frac{1 + C_3}{2}e^{-nH} + \frac{2\sigma_{1n}\sigma_{2n}}{C_3}\right]\right\}, \quad (5)$$

where (Belaya et al., 1994b)

$$\sigma_n = [\sigma\, cn(nl) + v\, nsh(nl)]e^{-nl}\left(1 - \frac{k}{n_0}\right). \quad (6)$$

In Eqs. 5 and 6, n is a measure of the decay length of nonlocal effects, $N(x) = (e^x - C_3^2\, e^{-x})/2$, and C_1, C_3 are constants. For reasonable values of the parameters it turns out that Eq. 5 only makes a significant contribution to the total force at separation distances of less than 2–3 nm.

Equation 3 is identical in form to an equation derived by Parsegian et al. for the electrostatic interaction energy between two surfaces with fixed charge densities σ_1 and σ_2. For the more general case considered above of a surface that has both a net charge density as well as a dipole density, the fixed charges in the equation are replaced by the appropriate effective charges. In both cases the interaction was obtained in the limit of small surface potential, so that the reduced surface potential $Z_S\, e\psi/k_BT \ll 1$.

COMPARISON WITH EXPERIMENTS

In our initial attempt we compared Eq. 3 with our experimental results. The effective surface charges were assumed to be constant and thus independent of the separation between the surfaces. For the Si_3N_4–Si_3N_4 case the charges on the tip were assumed to be the same as those on the flat substrate. The inverse Debye length, k, was calculated from the ion concentration for the 1:1 KCl electrolyte, and the tip radius was determined by the procedure outlined below. The surface charge density was left as an adjustable parameter. For the asymmetrical lipid–Si_3N_4 case, the charge density on the Si_3N_4 tip was as determined for the Si_3N_4–Si_3N_4 case, and the effective charge on the lipid was the adjustable parameter. For the lipid–lipid experiment, the effective charge on both lipid layers was assumed to be equal and served as an adjustable parameter.

To compare experimental data with theoretical models, it is essential that the shape of the AFM tip be known. Detailed tip characterization can be avoided if an effective tip radius is determined by calibrating the system with spherical tips of known radius that are attached to the cantilevers (Drummond and Senden, 1994; Senden and Drummond, 1995). This should provide a valid characterization for distances that are large compared to the inevitable surface roughness of the spheres. In our experiment we hoped to obtain more detailed information about the tip by scanning the tip over a variety of known shapes. Tips were scanned over polystyrene spheres of 225 nm diameter, over 300–700-nm-wide rectangular grooves cut into a GaAs substrate, and over 10-nm-thick fibers. A tip profile capable of reproducing the cross sections of all three shapes was then deduced. The resulting tip profile is shown in the inset in Fig. 8. From this figure it is still difficult to decide what value to take for the tip radius. We therefore used the approach suggested by Drummond and Senden (1994) for the determination of an effective tip radius. We measured the repulsive force between Si_3N_4 surfaces at a pH of 10. From the magnitude of the force at a separation of 10 nm we obtained from their figure 10 a value of ~250 nm for the

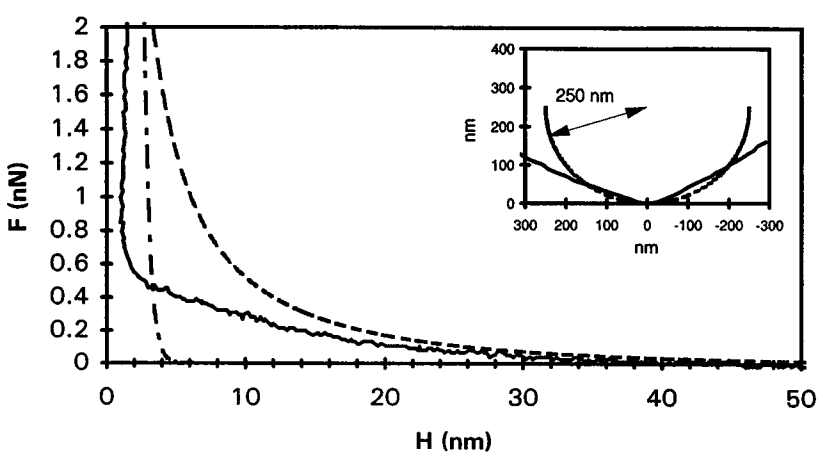

FIGURE 8 Comparison of Eq. 3 with the approach curve for lipid-coated surfaces. The figure shows the repulsive force as function of the separation distance H between the interacting charge planes. The solid line is the experimental data from Fig. 6 *b*. Negative charges were assumed to be located on the lipid at the boundary between the polar heads and the hydrocarbon tails. Hard surface contact was taken to occur when the polar heads from the opposing surfaces touched. The maximum thickness of the polar heads is about 0.5 nm, and the experimental curve was therefore displaced from the origin by 1 nm. The dashed line is Eq. 3 for a tip radius of 250 nm and a total charge density on each lipid surface of 0.0025 C/m^2. The dash-dot line is Eq. 5 for a surface dipole density $v = 1.8 \times 10^{-10}$ C/m and range parameter $n = 0.4$ nm. The inset shows a comparison of the effective tip (*dotted line*) with the tip profile that was deduced from the AFM images of a variety of structures (*solid line*).

effective tip radius. This radius is also shown in the inset in Fig. 8. Our measurements thus confirm the earlier observation of Drummond and Senden (1994) that the effective tip radius needed for force measurements in an electrolyte can be considerably larger than the geometrical radius of the tip apex.

Comparison with theoretical models also requires a knowledge of the location of the hard surfaces that define the contact between sample and tip and hence define the zero for the separation distance. For the lipid-coated surfaces contact was assumed to take place when the polar heads of the lipids touched the opposing surface that consisted either of Si_3N_4 (for the lipid–Si_3N_4 experiment) or of polar heads (for the lipid–lipid experiment). As discussed below, Cl^- counter-ion binding to the positively charged amine ends of the polar heads could lead to net charges residing on the lipids. The real surface charges (as well as the effective charges) on the lipids were assumed to be located at the negatively charged oxygen end of the polar heads. For the comparison with Eq. 3 the separation distances for the force curves were therefore corrected for the thickness of the polar head layer, which is 0.5 nm at most.

Fig. 8 shows a comparison of Eq. 3 (*dashed line*) with experimental results for a tip with an effective radius of 250 nm. It is evident from Fig. 8 that a reasonable fit can be obtained for large separation distances, but that the theoretical curve is progressively above the experimental one at short distances. For the Si_3N_4–Si_3N_4 case such a comparison is only meaningful down to about 15 nm. Below this distance an attractive force starts to dominate and produces the observed tip instability. This attractive force, which may, at least in part, have a van der Waals origin, appears to be very weak in the experiments that involved the lipid films. The charge densities derived from a comparison of the data for the various surface combinations with the linearized theory are in the range of 0.002–0.006 C/m^2. This implies a charge in the range of one electron in a 6.5 × 6.5 nm^2 area.

If we use the Grahame equation for the surface potential of a charged surface in a 1:1 electrolyte, we find that, for the above charge densities, $e\psi/k_bT > 1$, and Eq. 3 may not be applicable to our data. To obtain a better comparison and to examine the size of the discrepancies introduced by Eq. 3, we also performed a numerical evaluation of an exact solution of the nonlinear Poisson-Boltzmann equation.

Fig. 9 is an example of this comparison for the symmetrical case of lipid facing lipid shown in Fig. 6. A surface charge density of 0.004 C/m^2 gives a reasonable fit down to about 6 nm. Below this the numerical results are progressively above the data, as was the case for the linearized solution. If we use a charge density of 0.004 C/m^2 in Eq. 3, then the calculated force is very much larger than the experimental data, as shown by the heavy dashed line in Fig. 9. Comparison of the numerical solution with the Si_3N_4–Si_3N_4 data of Fig. 1 *b* above the tip instability region gave a surface charge of 0.009 C/m^2, with the theoretical curve again being progressively above the experimental one at shorter distances. The surface charge deduced for the Si_3N_4 is thus somewhat larger than that for the lipid surfaces.

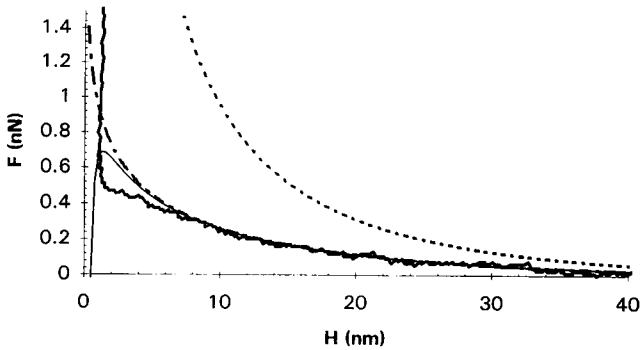

FIGURE 9 Comparison of the lipid-lipid data of Fig. 6 *b* with the exact solution of the Poisson-Boltzmann equation. The thick solid line is the experimental data (retraction curve). The experimental results have been shifted away from the origin by 1 nm, as discussed in connection with Fig. 8. The dash-dot line is the exact result for a charge density of 0.004 C/m^2, a tip radius of 250 nm, and a Debye length of 14 nm. Below ~7 nm the exact solution deviates considerably from the experimental data. The thin solid line is the exact solution with a van der Waals term with a Hamaker constant $A = 7 \times 10^{-21}$ J subtracted. Including the van der Waals term does not produce a substantial improvement of the fit at short distances. The dotted line is Eq. 3 with a surface charge density of 0.004 C/m^2 and a tip radius of 250 nm.

The deviation of the theoretical curves from the experimental data at short separation distances may suggest that an attractive force component becomes important in this region. The Hamaker constant, A, for Si_3N_4-water-Si_3N_4 was calculated by Senden and Drummond (1995) to be 6.07×10^{-20} J. For a sphere of radius R a distance d away from a flat plate, the van der Waals force (Israelachvili, 1985) is generally taken to be $F_{vw} = AR/6d^2$. For the tip radius of 250 nm and with the above Hamaker constant, the attractive force component is too small to account for the deviation of the data from the theoretical Coulomb term. Within the Derjaguin approximation both the Coulomb term and the van der Waals term are proportional to the tip radius, so that the observed discrepancy cannot be removed by taking a larger tip radius. For the lipid–lipid data the Hamaker constant (Marra and Israelachvili, 1985) may be taken to be an order of magnitude smaller than that for Si_3N_4–Si_3N_4; the net interaction force for $A = 7 \times 10^{-21}$ J is shown in Fig. 9 as the thin solid line. Although the agreement with the data can be improved with this term near the 2 nm region, the characteristic tip instability signature appears to be absent.

A much larger long-range attractive force was recently shown to be acting on neutral surfaces immersed in an electrolyte (Spalla and Belloni, 1995; Kekicheff and Spalla, 1995). The origin of this force is the correlation of charge fluctuations between the nominally neutral surfaces. These charge fluctuations and the resulting long-range forces were discussed for hard surfaces. It is not clear at present to what extent these results are applicable to our lipid experiments and hence to the soft interfaces we studied. It would seem, however, that the charge fluctuation problem will be considerably more difficult to treat theoretically for zwitterionic sur-

faces, and the relevance of this long-range attractive force for our force measurements remains unclear at present.

An alternative explanation of the discrepancy between the data and the Poisson-Boltzman solution may be a variation in the charge on the surfaces as the separation distance decreases. It is likely that neither the surface charge nor the surface potential remains constant as the surfaces approach. If we assume that the electrostatic interaction dominates the observed force curves, then we can deduce the surface charge at a particular separation distance from constant charge solutions to the equations by adjusting the charges on the surfaces to give agreement with the data at each separation distance. The resulting variation of surface charge with distance for the exact solution of the Poisson-Boltzmann equation for the lipid–lipid data is given in Fig. 10. The surface charge thus calculated is approximately constant down to the Debye length and then decreases by about 30% as the surfaces approach ~4 nm. A similar but more pronounced decrease in the surface charge is calculated with Eq. 3, because the linearized solution gives a larger force at short distances. This behavior is similar to the charge regulation for 1:1 electrolytes discussed some time ago by Chan et al. (1975). In their calculations the surface charge is nearly constant to separation distances near the Debye length and then decreases to very small values as the surfaces come into close contact.

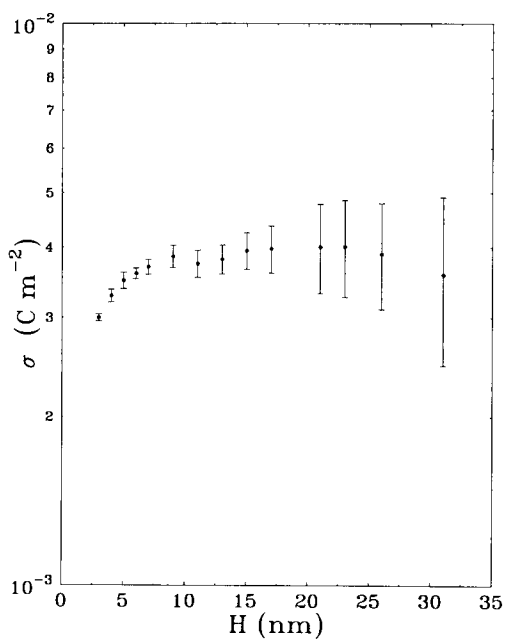

FIGURE 10 Surface charge as function of separation distance for the lipid-lipid data of Fig. 6 *b*. The discrepancy between the exact solution and the data below 7 nm might be explained if the surface charge were to decrease as the surfaces approach. The variation of surface charge shown was obtained by adjusting σ at a given separation until the exact solution of the Poisson-Boltzmann equation for the force agreed with the experimental value. Without the 1-nm offset of the data, the discrepancy between the exact solution and the experiment is larger and a somewhat larger charge variation with separation distance is obtained.

The validity of this proposed charge regulation ultimately depends on the detailed mechanisms that are responsible for the surface charges on the Si_3N_4 as well as on the lipid surfaces. Harame et al. (1987) and Grattarola et al. (1992), for example, have used a two-site theory to explain the formation of the potential and charge at the Si_3N_4 surface in electrolyte. The state of charge of the hydrolyzed Si_3N_4 surface was also discussed by Senden and Drummond (1995), and it was suggested that the surface charge is strongly influenced by anion (Cl^- in our case) complexion to the silylammonium groups on the Si_3N_4 surface. The counter-ion binding of these groups will thus determine the net charge density bound to the surface. The situation for the lipid surfaces may be similar. Although DMPC is a nominally neutral surface, Cl^- binding to the positively charged ends of the headgroups may dominate the binding of Na^+ to the oxygen end of the lipid dipole, thus giving the surface a net negative charge. Preferential ion binding to zwitterionic surfactants was also demonstrated by Kamenka et al. (1995). The mechanism for the charge regulation in the case of counter-ion binding, particularly to zwitterionic surfaces, clearly needs further study. If counter-ion binding is the dominant charging mechanism for our surfaces in an electrolyte, then because the electrolyte is added after the lipid layers are deposited, the charges responsible for the measured interaction may then reside principally on the sample surface that is in contact with the electrolyte, and it is then appropriate to neglect charges at the SiN-lipid surface as we have done for our analysis.

The calculated charge in 0.5 mM KCl electrolyte is 0.004 C/m^2 for the lipid–lipid experiment. In the spirit of Eq. 4, this net charge should contain a true surface charge plus an effective charge that arises from the perpendicular component of the surface dipoles. With an average area per DMPC molecule of 0.45 nm^2 and a charge separation distance in the dipole of 0.5 nm, we obtain a dipole moment density ν of 1.8×10^{-10} C/m if the dipoles are oriented perpendicular to the surface. The maximum value of the second term in Eq. 4 is then 4.5×10^{-4} C/m^2. It is likely that the dipoles are oriented more nearly parallel to the surface, and for an angle of 20°, for example, the effective charge is 1.5×10^{-4} C/m^2. With a net observed charge of ~0.004 C/m^2 the dipole contribution thus seems too small to have a significant effect. The dipole contribution could be increased by going to higher salt concentrations and thus shorter Debye lengths. Thus the dipole contribution could be made comparable to the net observed charge by going to a Debye length on the order of 1 nm. At such a short length, however, so many other contributions to the force come into play that it will be difficult to separate out the Coulomb components. This is already clear from our measurements for 50 mM KCl electrolyte in Fig. 7. A further complication could arise from the nonlocal term in Eq. 5. For parameters appropriate for our lipid experiments the nonlocal term in Eq. 5 is negligible down to separations of a few nanometers. The nonlocal force then rises very sharply, as shown in Fig. 8. If this term exists, it would be difficult to distinguish this

contribution from hydration forces and it would make the location of the sample surface in our type of experiment uncertain up to 1 nm.

The numerical force calculation shows that the interaction force saturates in the limit of large surface charges. This is illustrated in Fig. 11, where the interaction energy per unit area of two flat plates at a separation distance of $2\lambda_D$ is plotted as function of the reduced surface potential at infinite plate separation, Z_s. At Z_s larger than 8 the interaction energy and hence force become very insensitive to the magnitude of the surface potential or to the charge on the surfaces. $Z_s = 8$ implies a surface potential of 200 mV or a surface charge of 0.06 C/m^2. The determination of surface charges from AFM force measurements is thus limited to surface charge densities considerably less than 0.1 C/m^2.

SUMMARY

We have used the AFM to measure the interaction force between DMPC lipid-coated surfaces immersed in KCl electrolyte and attempted a detailed comparison of the data with a number of theoretical models for the electrostatic interaction. Although the lipids were nominally neutral, a long-range repulsive force was measured over lipid surfaces. A comparison of the data with exact solutions of the Poisson-Boltsmann equation gave a net surface charge on the lipid of 0.004 C/m^2, or about one electron charge per 100 lipid molecules. At separation distances of less than 7 nm, the exact solutions were consistently above the experimental curves. One possible interpretation of this deviation is a surface charge that decreases as the surfaces come into close proximity. The radius of the AFM tip is the most uncertain parameter in our calculations. This uncertainty may affect the overall magnitude of the surface charge but should have a minor effect on such aspects as the charge regulation mentioned above. For the surface charges and hence surface potentials encountered, the solution of the linearized Poisson-Boltzmann equation gave a considerable overestimate of the interaction force. This form of the solution can thus only be applied if the surface potential is considerably less than 25 meV. We were unable to verify recent predictions about effective surface charges that may arise for surface dipoles at soft interfaces or the predictions about nonlocal electrostatic forces at short separation distances.

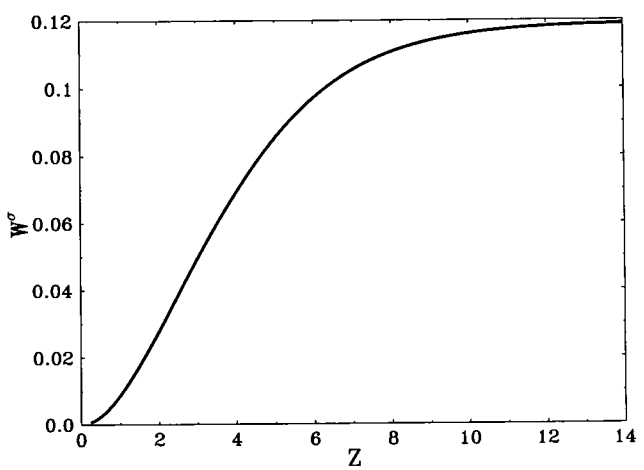

FIGURE 11 Plot of the theoretical interaction energy per unit area, W_σ, for flat plates at a separation distance of $2\lambda_D$ as a function of the reduced surface potential at infinite plate separation, Z_s. For $Z_s > 8$ the ion density and hence the repulsive force are insensitive to the magnitude of the surface charges, and force curves cannot give reliable information about surface charges.

REFERENCES

Belaya, M. L., M. V. Feigel'man, and V. G. Levadny. 1987. Structural forces as a result of nonlocal water polarizability. *Langmuir.* 3:648–654.

Belaya, M., V. Levadny, and D. A. Pink. 1994a. Electric double layer near soft permeable interfaces. 1. Local elestrostatics. *Langmuir.* 10: 2010–2014.

Belaya, M., V. Levadny, and D. A. Pink. 1994b. Electric double layer near soft permeable interfaces. 2. "Nonlocal" theory. *Langmuir.* 10:2015–2024.

Butt, H. J. 1991a. Measuring electrostatic, van der Waals, and hydration forces in electrolyte solutions with an atomic force microscope. *Biophys. J.* 60:1438–1444.

Butt, H. J. 1991b. Electrostatic interaction in atomic force microscopy. *Biophys. J.* 60:777–785.

Butt, H. J. 1995. Measuring surface forces in aqueous electrolyte solution with the atomic force microscope. *Biochem. Bioenerg.* 38:191–201.

Chan, D., J. W. Perram, L. R. White, and T. W. Healy. 1975. Regulation of surface potential at amphoteric surfaces during particle-particle interaction. *J. Chem. Soc. Farad. Trans. I.* 71:1046–1057.

Cleveland, J. P., S. Manne, D. Bocek, and P. K. Hansma. 1993. A nondestructive method for determining the spring constant of cantilevers for scanning force microscopy. *Rev. Sci. Instrum.* 64:403–405.

Ducker, W. A., T. J. Senden, and R. M. Pashley. 1991. Direct measurement of colloidal forces using an atomic force microscope. *Nature.* 353: 239–241.

Drummond, C. J., and T. J. Senden. 1994. Examination of the geometry of long-range tip- sample interaction in atomic force microscopy. *Colloids Surfaces A.* 87:217–234.

Grattarola, M., G. Massobrid, and S. Martinoia. 1992. Modeling H^+-sensitive FET's with SPICE. *IEEE Trans. Electron. Devices.* 39:813–819.

Harame, D. L., L. J. Bousse, J. D. Shott, and J. D. Meindl. 1987. Ion-sensing devices with silicon nitride and borosilicate glass insulators. *IEEE Trans. Electron. Devices.* 34:1700–1707.

Honig, E. P., and P. M. Mul. 1971. Tables and equations of the diffuse double layer repulsion at constant potential and constant charge. *J. Colloid Sci.* 36:258–272.

Israelachvili, J. N. 1985. Intermolecular and Surface Forces. Academic Press, London.

Kamenka, N., M. Chorro, Y. Chevallier, H. Levy, and R. Zana. 1995. Aqueous solutions of zwitterionic surfactants with varying carbon number of the intercharge group. 2. Ion binding by micelles. *Langmuir.* 11:4234–4240.

Kekicheff, P., and O. Spalla. 1995. Long-range electrostatic attraction between similar, charge-neutral walls. *Phys. Rev. Lett.* 75:1851–1854.

Levatny, V. G., M. L. Belaya, D. A. Pink, and M. H. Jericho. 1996. Theory of electrostatic effects in soft biological interfaces using atomic force microscopy. *Biophys. J.* 70:1745–1752.

Marra, J., and J. N. Israelachvili. 1985. Direct measurements of forces between phosphatidylcholine and phosphatidylethanolamine bilayers in aqueous electrolyte solutions. *Biochemistry.* 24:4608–4618.

Parsegian, V. A., and D. Gingell. 1972. On the electrostatic interaction across a salt solution between two bodies bearing unequal charges. *Biophys. J.* 12:1192–1204.

Rädler, J., M. Radmacher, and H. E. Gaub. 1994. Velocity-dependent forces in atomic force microscopy imaging of lipid films. *Langmuir.* 10:3111–3115.

Senden, T. J., and C. J. Drummond. 1995. Surface chemistry and tip-sample interaction in atomic force microscopy. *Colloids Surfaces A.* 94:29–51.

Spella, O., and L. Belloni. Long-range electrostatic attraction between neutral surfaces. *Phys. Rev. Lett.* 74:2515–2518.

Verwey, E. J. W., and J. T. G. Overbeek. 1948. Theory of Stability of Lyotropic Colloids. Elsevier, Amsterdam.

Weisenhorn, A. L., P. Maivald, H.-J. Butt, and P. K. Hansma. 1992. Measuring adhesion, attraction, and repulsion between surfaces in liquids with an atomic force microscope. *Phys. Rev. B.* 45:11226–11232.

White, L. R. 1983. On the Deryaguin approximation for the interaction of macrobodies. *J. Colloid Interface Sci.* 95:288.